Biosensors and Bioelectronics 128 (2019) 45–51

Contents lists available at ScienceDirect

Biosensors and Bioelectronics

journal homepage: www.elsevier.com/locate/bios

A signal-on magnetic electrochemical immunosensor for ultra-sensitive detection of saxitoxin using palladium-doped graphitic carbon nitride-based non-competitive strategy

Xin Jin[a], Jianlang Chen[a], Xiaoxue Zeng[a], LiangJun Xu[a], Yongning Wu[b], FengFu Fu[a,*]

[a] Key Laboratory for Analytical Science of Food Safety and Biology of MOE, Fujian Provincial Key Lab of Analysis and Detection for Food Safety, College of Chemistry, Fuzhou University, Fuzhou, Fujian 350116, China
[b] China National Center for Food Safety Risk Assessment, Beijing 100022, China

ARTICLE INFO

Keywords:
Shellfish toxins
Graphitic carbon nitride
Enzyme mimetics
Shellfish
Seawater
Seafood

ABSTRACT

Saxitoxin (STX) has high toxicity, and is water soluble, acid stable and thermostable. Therefore, STX in seawater can be accumulated by marine organism to form bioaccumulation. To ensure the safety of seafood for consumption, it is crucial to accurately determine trace STX in seawater and seafood. We herein developed a novel magnetic electrochemical immunosensor for ultra-sensitive detection of STX in seawater and seafood by using non-competitive strategy. The immunosensor employs STX-specific antibody-functionalized magnetic beads (MBs) for STX recognition, palladium-doped graphitic carbon nitride (g-C_3N_4-PdNPs) peroxidase mimetic for catalyzing H_2O_2-mediated oxidation of 3,3',5,5'-tetramethylbenzidine (TMB) to generate signal. The immunosensor combines the merits of g-C_3N_4-PdNPs peroxidase mimetic, non-competitive strategy, MBs-based antibody recognition and magnetic gold electrode, and thus has excellent stability, lower cost, no risk of false positive result, high sensitivity and strong ability resist to matrix interference. The proposed immunosensor has been successfully used to detect trace STX in seawater and shellfish samples with a detection limit of 1.2 pg/mL (4.0×10^{-12} M), a recovery of 93–107% and a relative standard deviation (RSD, n = 5) < 5%. The success of this study provided a promising approach for the rapid and on-site detection of trace STX in seawater and seafood.

1. Introduction

The paralytic shellfish toxins (PSTs) are a group of naturally occurring neurotoxic alkaloids, which primarily produced by the marine dinoflagellates and freshwater cyanobacteria (Abi-Khalil et al., 2017; Wiese et al., 2010). Among all PSTs, the saxitoxin (STX) is the most researched one to date since it is the only marine natural product classified as a Schedule I Chemical Warfare Agents per the Chemical Weapons Convention of 1993 (Cusick and Sayler, 2013). It was well known, STX is water soluble, acid stable and thermostable (Abi-Khalil et al., 2017), and therefore the STX in water can be accumulated by aquatic organism to form serious bioaccumulation. It was reported that consumption of STX-contaminated seafood may result in fatal illness such as respiratory arrest, cardiovas-cular shock and even the death of the seafood consumer in extreme cases (Abi-Khalil et al., 2017; Landsberg et al., 2006; Shin et al., 2017). For above reasons, a guideline of 7.5 μg STX equivalents/100 g seafood has been suggested by the European Food Safety Authority EFSA to ensure the safety of seafood (Etheridge, 2010). In order to control the effectiveness of these legal provisions and ensure the safety of seafood for consumption, it is crucial to accurately determine trace STX in aqueous environment especially in seawater and seafood.

Currently, the main techniques used for STX detection in seafood have capillary electrophoresis (CE) (Keyon et al., 2014a, 2014b), liquid chromatography (LC) and liquid chromatography-mass spectrometry (LC-MS) (Blay et al., 2011; Boundy et al., 2015; Bustillos-Guzmán et al., 2015; Harju et al., 2015; Jansson and Åstot, 2015; Mattarozzi et al., 2016; Watanabe et al., 2013; Zhuo et al., 2013). These methods have better accuracy. However, these methods required sophisticated and expensive equipment, complicated pre-treatment and skillful technician, which make the on-site and rapid detection of STX impossible. Especially, these methods have lower sensitivity, and thus cannot be used to detect ultra-trace STX in seawater directly. To realize the on-site detection of trace STX, a variety of methods including surface-enhanced Raman scattering (SERS) (Müller et al., 2014; Olson et al., 2011), enzyme-linked immunosorbent assays (ELISA) (Chu et al., 1996; Kawatsu

* Corresponding author.
E-mail address: fengfu@fzu.edu.cn (F. Fu).

https://doi.org/10.1016/j.bios.2018.12.036
Received 26 October 2018; Received in revised form 15 December 2018; Accepted 17 December 2018
Available online 26 December 2018
0956-5663/

et al., 2014; Wharton et al., 2017), electrochemical aptasensor (Hou et al., 2016), and a variety of immunosensors have been developed (Fraga et al., 2012, 2013; Haughey et al., 2011; Kim and Choi, 2015; Meneely et al., 2013; Szkola et al., 2013, 2014; van den Top et al., 2011; Yakes et al., 2011). Among all above methods, SERS has poorer sensitivity and specificity, and also needs expensive equipment, whereas, electrochemical aptasensor has poor stability and poor ability resist to complex matrix such as seawater. The ELISA and immunosensors previously reported all employed competitive strategy, which need natural enzyme-labeled STX and thus have poorer stability, higher cost and risk of false positive result. Therefore, these methods cannot be used for the direct and rapid detection of ultra-trace STX in water containing high salinity such as seawater in situ. In comparison with competitive STX immunoassay, the non-competitive STX immunosensor has obvious analytical advantages such as signal-on, no risk of false positive result and better stability due to no usage of natural enzyme. Thus, it is of great significance to develop a non-competitive immunosensor for the specific, sensitive and rapid detection of trace STX in seawater and seafood.

Artificial enzyme mimetic especially nano-material enzyme mimetic not only have catalytic activities with high efficiency and selectivity similar to natural enzyme but also have other excellent advantages including tunable structure, high stability, lower cost and easy modification in comparison with natural enzyme (Gao and Yang, 2006; Kuah et al., 2016), and thus have attracted increasing attention in recent years (Gao et al., 2007; Lin et al., 2014; Song et al., 2010; Vázquez-González et al., 2017; Wang et al., 2017; Wei and Wang, 2008). Lately, we reported a novel nano-material peroxidase mimetic, palladium-doped graphitic carbon nitride nano-sheets (g-C_3N_4-PdNPs), and demonstrated that it possesses higher intrinsic peroxidase-like activity and can effectively catalyze H_2O_2-mediated oxidation of 3,3',5,5'-tetramethylbenzidine (TMB) (Jin et al., 2018). Magnetic beads (MBs) can be easily collected with a magnet, and thus has been widely used as a carrier for the pre-concentration or specific capture of different molecules in sensing system to improve the sensitivity and the resistibility against matrix interference of the method (Wang et al., 2013; Zhang et al., 2013). Stimulated by above results, we herein developed a signal-on electrochemical immunosensor for the ultra-sensitive and specific detection of trace STX in seawater and seafood based on magnetic gold electrode (MGE), antibody-functionalized MBs and g-C_3N_4-PdNPs peroxidase mimetic-based non-competitive strategy. The combination of the MGE, non-competitive strategy and MBs-based g-C_3N_4-PdNPs catalytic amplification provides an ultra-high sensitivity, better specificity, excellent stability and strong ability resist to complex matrix, which makes the on-site determination of trace STX in seawater and seafood possible.

2. Experimental section

2.1. Materials and apparatus

The palladium-doped graphitic carbon nitride nano-sheets (g-C_3N_4-PdNPs), which possess peroxidase-like activity, were prepared according to previous method (details see Supporting information, SI) and used in experiment directly within 3 months (Jin et al., 2018). The prepared g-C_3N_4-PdNPs are laminated structure, and there are 10 nm-sized palladium nanoparticles with obvious crystal stripe (PdNPs) uniformly mono-dispersing on the surface (see Fig. 1). Streptavidin-modified magnetic beads (MBs, 1 μm, 10 mg/mL) were purchased from Invitrogen Technology Co., Ltd. (Oslo, Norway). Biotin-modified goat-anti-rabbit IgG secondary antibody (SA) and bovine serum albumin (BSA) was purchased from Boosen Biotechnology Co., Ltd. (Beijing, China). Saxitoxin (STX) standard and STX-specific antibody (Ab) were obtained from Express Technology Development Co., Ltd. (Beijing, China). The 10 mM TMB (3,3',5,5'-tetramethylbenzidine)-50 mM H_2O_2 solution were purchased from Neogen Inc. (USA). Milli-Q water

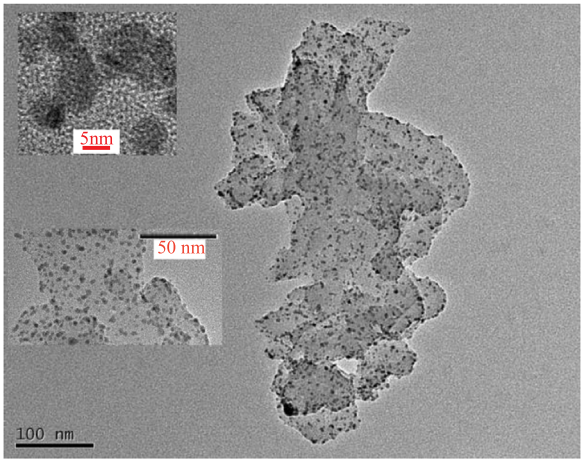

Fig. 1. The TEM images of the palladium-doped graphitic carbon nitride nano-sheets (g-C_3N_4-PdNPs), which was used as peroxidase mimetic in the experiment.

(18.2 MΩ cm) was used in all experiments. The buffers used in the experiment are as follow: PBS buffer (10 mM, pH 7.4) is the mixture of 135 mM NaCl, 3 mM KCl, 10 mM Na_2HPO_4 and 2 mM KH_2PO_4; PBS-T buffer (10 mM, pH = 7.4) is above PBS buffer containing 0.05% Tween-20; Tris-HCl buffer (10 mM, pH 7.0) was prepared by dissolving 0.30295 g Tris and 75 μL of 12 M HCl in 500 mL Milli-Q water and then adjusted pH to 7.0.

The magnetic gold electrode (MGE, diameter 3 mm) used in the experiment was purchased from Tianjin Incole Technology Co., Ltd (China), and a CHI-660C electrochemical workstation (CH Instrument, USA) was used for all electrochemical measurements.

2.2. Preparation of MBs/secondary antibody/STX-specific antibody/STX/g-C_3N_4-PdNPs conjugate

Firstly, 12.5 μL of 10 mg/mL MBs were washed with 200 μL of PBS-T buffer (pH 7.4) for 3 times under a magnet. Subsequently, 200 μL of 1000-folds diluted goat-anti-rabbit second antibody (SA) solution (in PBS-T buffer, pH 7.4) was added, and then the mixture was incubated for 30 min at room temperature to assemble SA on the MBs surface via the streptavidin-biotin specific interaction. The obtained SA-functionalized MBs (MBs/SA) were further treated with 200 μL of 2% BSA (dissolved in PBS-T buffer, pH 7.4) for 1 h at room temperature to block the space site of MBs surface in order to reduce non-specific adsorption. After washing with 200 μL of PBS-T buffer (pH 7.4) for 3 times, the MBs/SA conjugates were mixed with 75 μL of STX-specific antibody (Ab) solution, 75 μL of STX standard solution or sample solution and 50 μL of PBS buffer (pH 7.4) for 30 min at room temperature to form MBs/SA/Ab/STX conjugates. The obtained MBs/SA/Ab/STX conjugates were washed for 3 times with 200 μL PBS-T buffer (pH 7.4) under an external magnet, then 60 μL of the prepared g-C_3N_4-PdNPs and 40 μL of Tris-HCl buffer (pH 7.0) were added, and the whole was incubated for 75 min at room temperature to obtain MBs/SA/Ab/STX/g-C_3N_4-PdNPs conjugates via the electrostatic adsorption between STX and g-C_3N_4-PdNPs. After washing with 200 μL PBS-T buffer (pH 7.0) for 3 times, the obtained MBs/SA/Ab/STX/g-C_3N_4-PdNPs conjugates were re-suspended in 25 μL of Tris-HCl buffer (pH 7.0) and used for the next electrochemical measurements.

2.3. Electrochemical measurements

The electrochemical system used MGE as working electrode, a platinum wire as counter electrode and an Ag/AgCl electrode as reference electrode. The MGE was previously polished with 0.05 μm alumina

powder to obtain mirror surface, followed by ultra-sonication in ethanol and Milli-Q water for 1 min respectively. After blowing dry with nitrogen, the MGE was used for electrochemical measurements. The electrochemical measurements were performed in the TMB-H_2O_2 solution. First, the above prepared MBs/SA/Ab/STX/g-C_3N_4-PdNPs conjugates were adsorbed on the surface of MGE, then, the whole three-electrode system was immersed into 600 μL of TMB-H_2O_2 solution. The cyclic voltammetry scanning (CVs) was carried out in the voltage range of 0 ~ + 0.8 V with a scanning rate of 100 mV/s, and the chronoamperometry was performed with incipient potential of + 0.2 V, the sample interval of 0.1 s and the experimental time of 100 s. All measurements were carried out at room temperature.

2.4. Detection of seawater and shellfish samples

Seawater collected from Xiapu, Fujian Province of China was firstly filtered through a 0.45 μm filter membrane, and then the STX in the seawater was directly detected with above method. For shellfish sample, firstly, STX in 0.1 g dried mussel powder was extracted with 5 mL of 80% (v/v) methanol solution for 10 min under ultra-sonication (Jansson and Åstot, 2015). Then, the extract was separated by centrifuging at 3000 rpm for 10 min. The residue was repeatedly extracted with 5 mL of 80% methanol again with the same manner, and twice extracts were merged together. The total extract was filtered through a 0.45 μm filter membrane, and the STX in extract was directly detected with above method. The seawater and mussel samples, which previously spiked with different concentrations of STX, were also detected with the same manner to obtain recoveries.

3. Results and discussions

3.1. The design of the strategy for non-competitive magnetic electrochemical immunosensor

It was well known, antibody (Ab) can simultaneously bind second antibody (SA) and target molecular with high affinity and specifically. Lately, it was reported that g-C_3N_4-PdNPs possesses high intrinsic peroxidase-like activity (Jin et al., 2018). Thus, a non-competitive magnetic electrochemical immunosensor was designed for the ultra-sensitive and rapid detection of STX by using antibody as recognition probe and g-C_3N_4-PdNPs peroxidase mimetic for catalyzing H_2O_2-mediated oxidation of TMB to generate signal. The detailed principle of the non-competitive magnetic electrochemical immunosensor was shown in Scheme 1. Firstly, the biotin-labeled SA was assembled on the surface of streptavidin-modified MBs via the specific interaction between biotin and streptavidin. The SA-functionalized MBs (MBs/SA) can specifically bind STX-specific Ab to form STX-specific Ab-modified MBs (MBs/SA/Ab), and the obtained MBs/SA/Ab conjugates can specifically capture STX molecule with high affinity to form "sandwich-like" MBs/SA/Ab/STX conjugates. In Tris-HCl buffer (pH 7.0), the MBs/SA/Ab/STX conjugates possess positive charges since STX (its chemical structure see Fig. S1 in SI) is a weak alkali molecule with an ionization constant (K_{a1}) of $10^{-8.2}$. Whereas, the g-C_3N_4-PdNPs peroxidase mimetic possesses negative charges in Tris-HCl buffer (pH 7.0) since the surface of g-C_3N_4-PdNPs was modified with citrate ion, which has an ionization constant (K_{a1}) of $10^{-3.13}$ (Jin et al., 2018). Therefore, in Tris-HCl buffer (pH 7.0), MBs/SA/Ab/STX conjugates can capture g-C_3N_4-PdNPs peroxidase mimetic via electrostatic adsorption to form MBs/SA/Ab/STX/g-C_3N_4-PdNPs conjugates. By adsorbing MBs/SA/Ab/STX/g-C_3N_4-PdNPs conjugates on the MGE surface and dipping the MGE into the TMB-H_2O_2 solution, g-C_3N_4-PdNPs can effectively catalyze the H_2O_2-mediated oxidation of TMB since it possesses higher intrinsic peroxidase-like activity (Jin et al., 2018), and thus giving rise to an increasing electrochemical current signal. The amount of g-C_3N_4-PdNPs attached on MBs surface is proportional to the content of the STX, in other words, the electrochemical current signal is proportional to the content of the STX. This provides a "signal-on" sensing platform for the sensitive and rapid detection of STX.

As reported in previous study, in comparison with natural horseradish peroxidase (HRP), g-C_3N_4-PdNPs peroxidase mimetic possesses much higher activity, better stability (it can keep a constant peroxidase-like activity within 3 months under 5 °C storage) and lower cost (Jin et al., 2018). Therefore, in comparison with previous competitive STX immunoassay, the proposed magnetic electrochemical immunosensor has noticeable advantages such as ultra-high sensitivity, better reproducibility, signal-on, no risk of false positive result, lower cost and strong ability resist to matrix interference since it combined the merits of MBs-based non-competitive strategy, MGE and g-C_3N_4-PdNPs catalytic amplification.

3.2. Characterization of non-competitive magnetic electrochemical immunosensor

To confirm the feasibility of our strategy, the CVs behavior of TMB-H_2O_2 solution was investigated in detail at different stages of immunosensor preparation. As Fig. 2 showed, the CVs curve obtained with bare MGE (curve a) showed two pairs of peaks ($E_{p,a1}$ = + 0.32 V, $E_{p,c1}$ = + 0.38 V, $E_{p,a2}$ = + 0.48 V and $E_{p,c2}$ = + 0.56 V, respectively), which corresponding to TMB's two reversible one-electron couples (namely $TMB \leftrightarrow TMB^+ + e^-$; $TMB^+ \leftrightarrow TMB^{2+} + e^-$) (Doménech et al., 2004). In fact, the H_2O_2-mediated oxidization of TMB is a slow reaction. However, in the presence of peroxidase or nano-material peroxidase mimetic such as g-C_3N_4-PdNPs, the peroxidase or the peroxidase mimetic will effectively catalyze H_2O_2 to oxidize TMB, and the oxidation rate of TMB was improved. As a result, the current signal at $E_{p,a1}$ and $E_{p,c2}$ was greatly increased and the current signal at $E_{p,c1}$ and $E_{p,a2}$ was decreased (Wang et al., 2013). As Fig. 2b and Fig. 2c showed, when bare MBs or MBs/SA/Ab/STX conjugates were adsorbed on MGE surface, there is a little increase in current signal at $E_{p,a1}$ and $E_{p,c2}$. This is because that MBs itself has weak intrinsic peroxidases-like activity and can slightly catalyze the H_2O_2-mediated oxidation of TMB (Wang et al., 2013). When MBs/SA/Ab/STX/g-C_3N_4-PdNPs conjugates were adsorbed on the MGE surface, it was observed that the current signal at $E_{p,a1}$ and $E_{p,c2}$ increased significantly and simultaneously TMB solution color change from colorless to blue. This is because that g-C_3N_4-PdNPs has high peroxidase-like activity and can effectively catalyze the H_2O_2-mediated oxidation of TMB. Above results forcefully verified that our strategy of detecting STX is feasible. The relationship between scan rate (ν) and the peak current of TMB at $E_{p,a1}$ = + 0.32 V was also investigated to comprehend the reaction kinetics. As showed in Fig. S2 (see SI), the peak current of TMB at $E_{p,a1}$ = + 0.32 V showed a good linear relationship with the square root of scan rate, indicating a diffusion-controlled quasi-reversible process.

The Zeta-potential measurements and electrochemical impedance spectra (EIS) measurements also validated that the immunosensor was successfully fabricated as we expected. As Fig. 3A showed, in Tris-HCl buffer (pH 7.0), bare MBs suspension has a + 40 mV Zeta potentials, whereas MBs/SA conjugates and MBs/SA/Ab conjugates have a − 105 mV and − 140 mV Zeta potentials respectively, indicating that secondary antibody and STX-specific antibody have been successfully assembled on MBs surface. The Zeta potential of MBs/SA/Ab/STX conjugates shifted to + 12 mV, which confirmed the capture of STX molecule on the MBs/SA/Ab surface since STX possesses positive charge under pH = 7.0. As we mentioned above, g-C_3N_4-PdNPs possesses negative charge under pH = 7.0 since there are citrate ion assembling on its surface (Jin et al., 2018). Therefore, the negative Zeta potential (-7 mV) was observed for MBs/SA/Ab/STX/g-C_3N_4-PdNPs, which confirmed that g-C_3N_4-PdNPs was successfully adsorbed on the MBs/SA/Ab/STX surface via electrostatic adsorption.

As EIS results shown in Fig. 3B, compare to bare MGE (curve a), MBs-modified MGE, MBs/SA-modified MGE and MBs/SA/Ab-modified MGE showed a remarkable increasing Ret (resistance of electron-

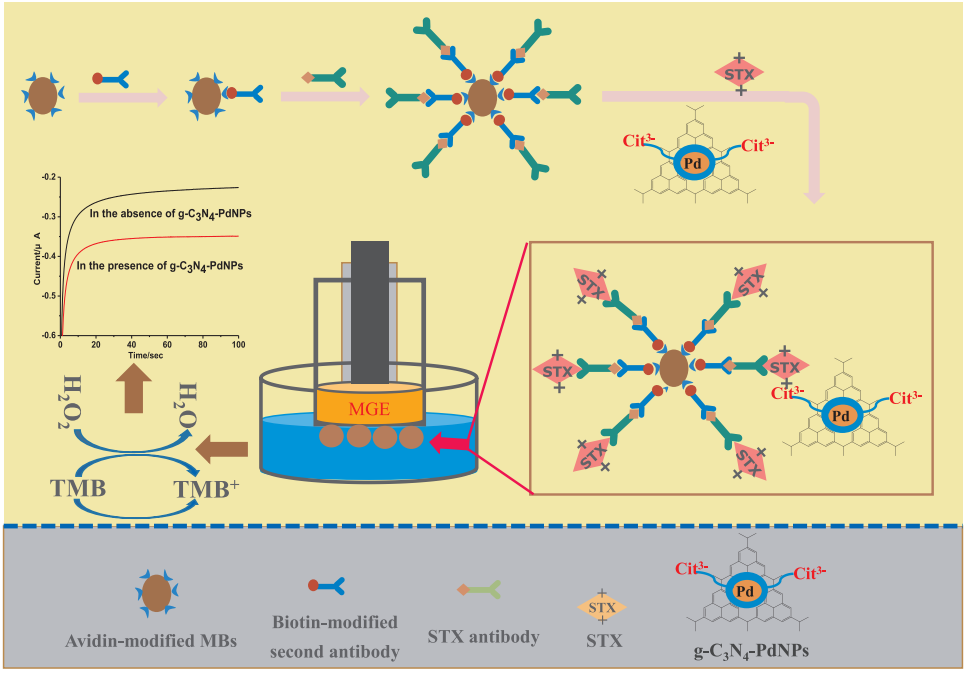

Scheme 1. The flow chart of the experimental strategy of non-competitive magnetic electrochemical immunosensor.

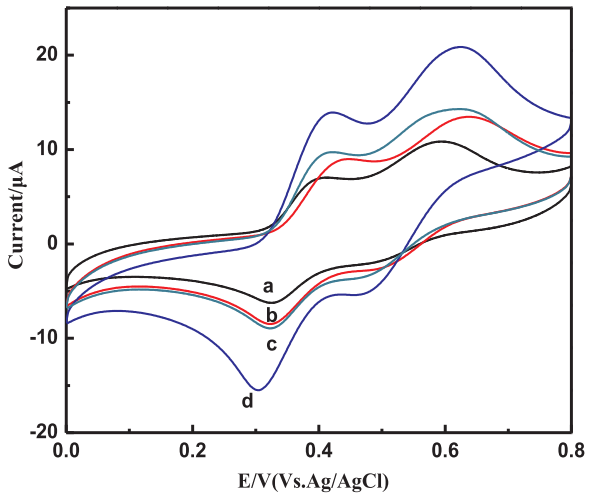

Fig. 2. The CVs of TMB-H_2O_2 solution at different electrode's surface. (a) bare MGE; (b) MGE adsorbed MBs; (c) MGE adsorbed MBs/SA/Ab/STX conjugates; (d) MGE adsorbed MBs/SA/Ab/STX/g-C_3N_4-PdNPs conjugates.

transfer) (curve b, c, d), indicating that secondary antibody and STX-specific antibody have been successfully assembled on MBs surface in sequence. However, in comparison with MBs/SA/Ab-modified MGE, MBs/SA/Ab/STX-modified MGE and MBs/SA/Ab/STX/g-C_3N_4-PdNPs-modified MGE showed a little smaller Ret (curve e, f) since MBs/SA/Ab/STX-modified MGE has an electro-positive surface and MBs/SA/Ab/STX/g-C_3N_4-PdNPs-modified MGE has a less electro-negative surface. The EIS results are consistent with those of Zeta-potential measurements, further confirmed that the non-competitive magnetic electrochemical immunosensor was successfully fabricated as we expected.

The X-ray photoelectron spectroscopy (XPS) analysis of MBs/SA/Ab/STX/g-C_3N_4-PdNPs conjugates showed a similar spectrum (see Fig. S3 in SI) to that of pure g-C_3N_4-PdNPs reported in previous study (Jin et al., 2018), which containing all C, N, Pd and O elements, further confirmed that the g-C_3N_4-PdNPs was successfully electrostatically adsorbed by MBs/SA/Ab/STX conjugates to form MBs/SA/Ab/STX/g-C_3N_4-PdNPs conjugates.

3.3. Optimization of the immunosensor's parameters

The MBs amount on the MGE surface directly affects the sensitivity of the method. In this study, the effect of the MBs amount on the sensitivity was investigated in detail in order to obtain the highest sensitivity. The experimental results (see Fig. S4 in SI) showed that the catalytic current of the TMB-H_2O_2 increased with the increasing of MBs amount in the range of 15–25 μg, then the catalytic current turn to decrease with the increasing of MBs amount when the MBs amount is more than 25 μg. This may be attributes to the bigger electron transfer resistance and steric hindrance caused by over MBs loadings. Therefore, 25 μg of MBs was used in the study.

The density of SA modified on the MBs surface affects the MBs/SA ability of binding STX-specific Ab, and thus affects the sensitivity of the method. The lower density of SA decreased the MBs/SA ability of binding STX-specific antibody, and thus harmed the sensitivity. Whereas, higher density of SA will increase electron transfer resistance, and thus harmed the sensitivity too. In this study, the density of SA modified on the MBs surface was controlled by controlling the dilution multiple of SA. As results shown in Fig. S5 (see SI), when the SA was diluted with 1000-folds, the immunosensor has a highest sensitivity and thus 1000-folds diluted SA was used in this study.

The dosage of STX-specific Ab directly affects the amount of STX-specific Ab bound on MBs/SA conjugates, and thus affects the MBs/SA/Ab conjugate's ability of binding STX, and finally affects the sensitivity of the immunosensor. Lower dosage of STX-specific Ab cannot provide adequate antibody for MBs/SA binding, which degrade the MBs/SA/Ab conjugate's ability of binding STX and finally degrade the sensitivity of the immunosensor. Higher dosage of STX-specific Ab will lead to the over loading of antibody, which increase electron transfer resistance and thus harmed the sensitivity too. Results shown in Fig. S6 (see SI) revealed that when 75 μL of STX-specific Ab was used, the immunosensor has a highest sensitivity and thus 75 μL of STX-specific Ab was used in this study.

The pH directly affects the ionization of STX molecules and citrate ions modified on the g-C_3N_4-PdNPs surface, and thus will affect the electrostatic adsorption between MBs/SA/Ab/STX conjugate and g-C_3N_4-PdNPs. To ensure STX molecules and g-C_3N_4-PdNPs possess different charges to generate electrostatic adsorption, the system pH was

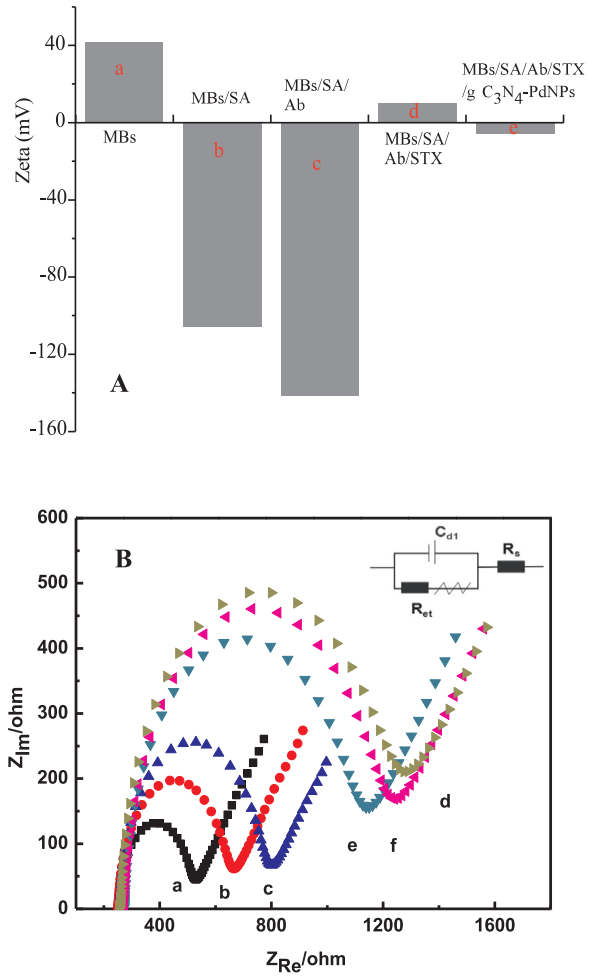

Fig. 3. A: The Zeta potential of bare MBs (a), MBs/SA conjugates (b), MBs/SA/Ab conjugates (c), MBs/SA/Ab/STX conjugates (d), and MBs/SA/Ab/STX/g-C_3N_4-PdNPs conjugates (e). B: Nyquist plots of EIS obtained in 10 mM Tris-HCl buffer-10 mM $[Fe(CN)_6]^{3-/4-}$ solution (pH 7.0) at different electrodes. (a) bare MGE; (b) MBs-modified MGE; (c) MBs/SA-modified MGE; (d) MBs/SA/Ab-modified MGE; (e) MBs/SA/Ab/STX-modified MGE; (f) MBs/SA/Ab/STX/g-C_3N_4-PdNPs-modified MGE.

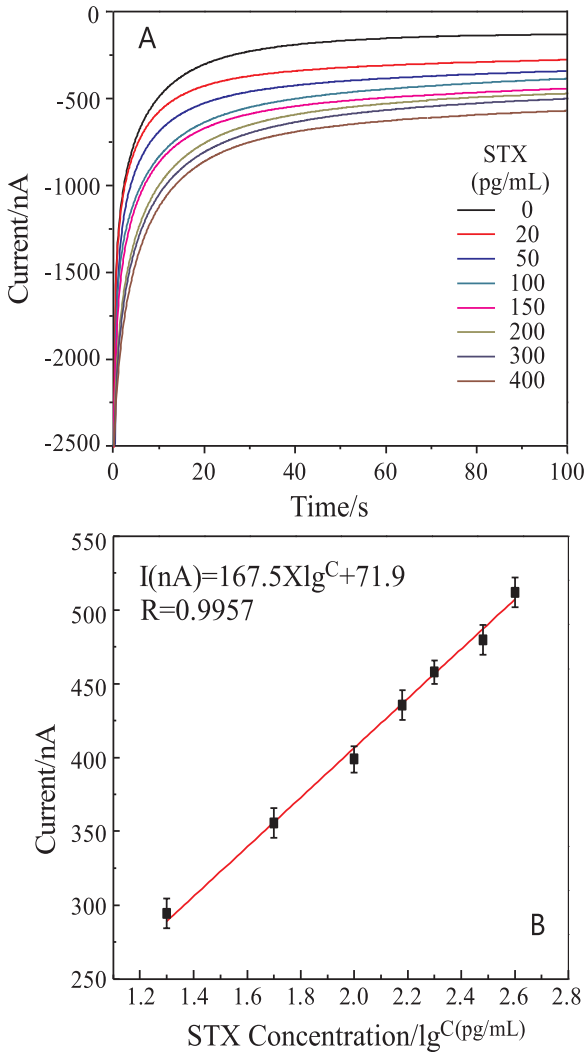

Fig. 4. A: Current-time curves for detecting different concentration of STX. From top to bottom, the concentration of STX increased from 0.0 pg/mL to 400 pg/mL. B: The linear relationship between the absolute value of net current and the logarithm of STX concentration.

controlled with Tris-HCl buffer and optimized in the range of 6.2–7.5 by referencing the ionization constant of STX ($K_{a1} = 10^{-8.2}$) and citric acid ($K_{a1} = 10^{-3.13}$). The results in Fig. S7 (see SI) revealed that there is a biggest electrostatic adsorption between electro-positive STX and electro-negative g-C_3N_4-PdNPs, and thus generate a biggest catalytic current when pH = 7.0. Therefore, the system was controlled at pH 7.0 with Tris-HCl buffer.

As a peroxidase mimetic, the dosage of g-C_3N_4-PdNPs nano-sheets directly affected the catalytic oxidation of TMB-H_2O_2, and finally affected the sensitivity of the method. As shown in Fig. S8 (see SI), the catalytic current increased upon the dosage of g-C_3N_4-PdNPs increasing in the range of 30–60 μL. Then, the catalytic current keeps almost no variation when the dosage of g-C_3N_4-PdNPs is larger than 60 μL. Thus, 60 μL of g-C_3N_4-PdNPs solution was used in the experiment.

The interaction time between MBs/SA/Ab/STX conjugates and g-C_3N_4-PdNPs will affect the amount of g-C_3N_4-PdNPs adsorbed on the surface of MBs/SA/Ab/STX, and thus will influence the catalytic current. Fig. S9 (see SI) revealed that the catalytic current increased with the increasing of interaction time when time is less than 75 min, and then the catalytic current turn to keep on constant level when time is longer than 75 min. To save analytical time, 75 min was selected as the optimal interaction time.

3.4. Analytical performance of non-competitive magnetic electrochemical immunosensor

Under the optimal conditions, the sensitivity and dynamic range of the non-competitive magnetic electrochemical immunosensor was investigated by detecting a series of STX standard solution with chronoamperometry. As shown in Fig. 4, the absolute value of catalytic current increased with the raise of STX concentration in the range of 20–400 pg/mL (6.7×10^{-11}–1.3×10^{-9} M), and the absolute value of net catalytic current (catalytic current after subtracting the background) showed a good linear correlation with the logarithm of STX concentrations (Fig. 4B). The regression equation was I (nA) $= 167.5 \times \log^C + 71.9$, with a correlation coefficient (R) = 0.9908, where C is STX concentration with the unit of pg/mL. The detection limit (3σ/S) for STX was calculated to be 1.2 pg/mL (4.0×10^{-12} M), and the relative standard deviation (RSD, n = 5) was calculated to be less than 5% for the detection of 50 pg/mL STX.

The specificity of the proposed immunosensor was investigated by detecting different shellfish toxins including domoic acid (DA), gonyautoxins (GTX 1–2), okadaic acid (OA) and saxitoxin (STX). As showed in Fig. S10 (in SI), only STX revealed a significant increasing current signal, whereas, the current signals of DA, GTX 1–2 and OA are

Table 1
Analytical results of STX in artificial seawater, real seawater and mussel samples.

Sample	[a]STX added	[b]Detected results	Recovery (%)	RSD (%)	[c]LC-MS/MS
Artificial seawater	0.0 pg/mL	[d] < DL	–	–	< DL
	50 pg/mL	48.7 pg/mL	94	5	< DL
	100 pg/mL	99.5 pg/mL	98	4	< DL
Seawater	0.0 pg/mL	2.3 pg/mL	–	5	< DL
	50 pg/mL	55.3 pg/mL	106	5	< DL
	100 pg/mL	106.5 pg/mL	104	4	< DL
Mussel	0.0 ng/g	0.65 ng/g	–	4	< DL
	1.0 ng/g	1.58 ng/g	93	5	1.53 ng/g
	2.0 ng/g	2.78 ng/g	107	3	2.65 ng/g

[a] STX concentrations added into artificial seawater, real seawater and mussel samples.
[b] STX concentrations in seawater and mussel detected with our method.
[c] STX concentrations in seawater and mussel detected with LC-MS/MS.
[d] STX concentration is lower than detection limit of the method.

approximatively the same as that of blank. Above results indicated that the proposed immunosensor has excellent specificity to STX.

3.5. Detection of seawater and seafood

To verify the reliability and feasibility of the proposed immunosensor to actual sample with complex matrix such as seawater and seafood, the artificial seawater was composed by adding 3% NaCl and different STX concentrations (0, 50 and 100 pg/mL) into Milli-Q water. Then, the STX concentrations in the artificial seawater were detected with the proposed immunosensor. As results in Table 1 revealed, the STX in artificial seawater was successfully detected with a recovery of 94–98% and a relative standard deviation (RSD) < 5% (n = 5), indicating that the proposed immunosensor has strong resistibility against complex matrix of sample. To further demonstrate the potential application of the proposed immunosensor, the STX in real seawater and mussel samples was detected with the proposed immunosensor. The seawater and mussel spiked with 50 and 100 pg/mL STX were also detected to obtain recovery. The results obtained with the proposed immunosensor were compared with those obtained with LC-MS/MS method (Zhuo et al., 2013), a traditional method for the STX detection. As results shown in Table 1, the seawater and mussel was detected to have a 2.3 pg/mL and 0.65 ng/g of STX respectively, with a recovery of 93–107% and a RSD (n = 5) < 5%. The results obtained with the proposed immunosensor are consistent with those obtained with LC-MS/MS method too. All above results revealed that our method is reliable and can be applied to the practical detection of STX in seawater and seafood.

So far, various methods including SERS, ELISA and several immunosensors have been developed for the rapid detection of STX (Chu et al., 1996; Fraga et al., 2012, 2013; Haughey et al., 2011; Hou et al., 2016; Kawatsu et al., 2014; Kim and Choi, 2015; Meneely et al., 2013; Müller et al., 2014; Olson et al., 2011; Szkola et al., 2013, 2014; van den Top et al., 2011; Wharton et al., 2017; Yakes et al., 2011). However, these methods suffer from one or more of following deficiencies, such as poorer specificity and sensitivity, poor resistibility against complex matrix, risk of false positive result and higher cost due to the employment of competitive strategy. In comparison with previous methods (see Table S1 in SI), the proposed non-competitive STX immunosensor has obvious analytical advantages such as much higher sensitivity, signal-on, lower cost and better reproducibility, no risk of false positive result and strong ability resist to complicated matrix since it combined the merits of MBs-based non-competitive strategy, MGE and g-C_3N_4-PdNPs peroxidase mimetic-based catalytic amplification. All above features make our method a promising approach for the on-site detection of STX in seawater and seafood.

4. Conclusions

In summary, we herein developed a novel signal-on magnetic electrochemical immunosensor for ultra-sensitive detection of STX in seawater and seafood by using antibody-modified MBs for specifically recognizing STX and g-C_3N_4-PdNPs peroxidase mimetic-based catalytic oxidation of TMB-H_2O_2 for signal generation. The proposed immunosensor has noticeable advantages including high sensitivity, better stability, lower cost, no risk of false positive result and strong resistibility against complex matrix since it combined the merits of non-competitive strategy, g-C_3N_4-PdNPs peroxidase mimetic, MBs and magnetic gold electrode. The proposed immunosensor has been successfully used to detect ultra-trace STX in seawater and seafood with a detection limit of 1.2 pg/mL (4.0×10^{-12} M), a recovery of 93–107% and a RSD (n = 5) < 5%. We believe that our strategy provided a promising approach for the on-site detection of trace STX in aqueous environment and seafood.

CRediT authorship contribution statement

Xin Jin: Investigation, Methodology. **Jianlang Chen:** Investigation, Methodology. **Xiaoxue Zeng:** Investigation, Methodology. **LiangJun Xu:** Formal analysis, Writing - review & editing. **Yongning Wu:** Formal analysis, Writing - review & editing. **FengFu Fu:** Conceptualization, Data curation, Formal analysis, Funding acquisition, Writing - original draft.

Acknowledgements

The authors gratefully acknowledge The National Key Research and Development Program of China (2017YFC1600500), NSFC (21677034) and the Program for Changjiang Scholars and Innovative Research Team in University (No. IRT-15R11) for financial support.

Appendix A. Supplementary material

Supplementary data associated with this article can be found in the online version at doi:10.1016/j.bios.2018.12.036.

References

Abi-Khalil, C., Finkelstein, D.S., Conejero, G., Bois, J.D., Destoumieux-Garzon, D., Rolland, J.L., 2017. Aquat. Toxicol. 190, 133–141.
Blay, P., Hui, J.P.M., Chang, J., Melanson, J.E., 2011. Anal. Bioanal. Chem. 400, 577–585.
Boundy, M.J., Selwood, A.I., Harwood, D.T., McNabb, P.S., Turner, A.D., 2015. J. Chromatogr. A 1387, 1–12.
Bustillos-Guzmán, J.J., Band-Schmidt, C.J., Durán-Riveroll, L.M., Hernández-Sandoval, F.E., López-Cortés, D.J., Núñez-Vázquez, E.J., Cembella, A., Krock, B., 2015. Food Addit. Contam.: Part A 32, 381–394.
Chu, F.S., Hsu, K.-H., Huang, X., Barrett, R., Allison, C., 1996. J. Agric. Food Chem. 44, 4043–4047.

Cusick, K.D., Sayler, G.S., 2013. Mar. Drugs 11, 991–1017.
Doménech, A., García, H., Casades, I., Esplá, M., 2004. J. Phys. Chem. B 108, 20064–20075.
Etheridge, S.M., 2010. Toxicon 56, 108–122.
Fraga, M., Vilariño, N., Louzao, M.C., Campbell, K., Elliott, C.T., Kawatsu, K., Vieytes, M.R., Botana, L.M., 2012. Anal. Chem. 84, 4350–4356.
Fraga, M., Vilariño, N., Louzao, M.C., Rodríguez, P., Camp-bell, K., Elliott, C.T., Botana, L.M., 2013. Anal. Chem. 85, 7794–7802.
Gao, L., Zhuang, J., Nie, L., Zhang, J., Zhang, Y., Gu, N., Wang, T., Feng, J., Yang, D., Perrett, S., 2007. Nat. Nanotechnol. 2, 577–583.
Gao, Z.Q., Yang, Z.C., 2006. Anal. Chem. 78, 1470–1477.
Harju, K., Rapinoja, M.-L., Avondet, M.-A., Arnold, W., Schär, M., Burrell, S., Luginbühl, W., Vanninen, P., 2015. Toxins 7, 4868–4880.
Haughey, S.A., Campbell, K., Yakes, B.J., Prezioso, S.M., DeGrasse, S.L., Kawatsu, K., Elliott, C.T., 2011. Talanta 85, 519–526.
Hou, L., Jiang, L.S., Song, Y.P., Ding, Y.H., Zhang, J.H., Wu, X.P., Tang, D.P., 2016. Microchim Acta 183, 1971–1980.
Jansson, D., Åstot, C., 2015. J. Chromatogr. A 1417, 41–48.
Jin, X., Zhong, Y.Y., Chen, L., Xu, L.J., Wu, Y.N., Fu, F.F., 2018. Part. Part. Syst. Charact. 35 (3), 1700359.
Kawatsu, K., Kanki, M., Harada, T., Kumeda, Y., 2014. Food Chem. 162, 94–98.
Keyon, A.S.A., Guijt, R.M., Gaspar, A., Kazarian, A.A., Nesterenko, P.N., Bolch, C.J., Breadmore, M.C., 2014a. Electrophoresis 35, 1496–1503.
Keyon, A.S.A., Guijt, R.M., Bolch, C.J.S., Breadmore, M.C., 2014b. J. Chromatogr. A 1364, 295–302.
Kim, M.-H., Choi, S.-J., 2015. Biosens. Bioelectron. 66, 136–140.
Kuah, E., Toh, S., Yee, J., Ma, Q., Gao, Z.Q., 2016. Chem. Eur. J. 22, 8404–8430.
Landsberg, J.H., Hall, S., Johannessen, J.N., White, K.D., Conrad, S.M., Abbott, J.P., et al., 2006. Environ. Health Perspect. 114, 1502–1507.
Lin, T.R., Zhong, L.S., Wang, J., Guo, L.Q., Wu, H.Y., Fu, F.F., Chen, G.N., 2014. Biosens. Bioelectron. 59, 89–93.
Mattarozzi, M., Milioli, M., Bianchi, F., Cavazza, A., Pigozzi, S., Milandri, A., Careri, M., 2016. Food Control 60, 138–145.
Meneely, J.P., Campbell, K., Greef, C., Lochhead, M.J., El-liott, C.T., 2013. Biosens. Bioelectron. 41, 691–697.
Müller, C., Glamuzina, B., Pozniak, I., Weber, K., Cialla, D., Popp, J., Pînzaru, S.C., 2014. Talanta 130, 108–115.
Olson, T.Y., Schwartzberg, A.M., Liu, J.L., Zhang, J.Z., 2011. Appl. Spectrosc. 65, 159–164.
Shin, H.H., Li, Z., Kim, E.S., Park, J.-W., Lim, W.A., 2017. Harmful Algae 68, 31–39.
Song, Y.J., Qu, K.G., Zhao, C., Ren, J.S., Qu, X.G., 2010. Adv. Mater. 22, 2206–2210.
Szkola, A., Campbell, K., Elliott, C.T., Niessner, R., Seidel, M., 2013. Anal. Chim. Acta 787, 211–218.
Szkola, A., Linares, E.M., Worbs, S., Dorner, B.G., Dietrich, R., Märtlbauer, E., Niessnera, R., Seidel, M., 2014. Analyst 139, 5885–5892.
van den Top, H.J., Elliott, C.T., Haughey, S.A., Vilariño, N., van Egmond, H.P., Botana, L.M., Campbell, K., 2011. Anal. Chem. 83, 4206–4213.
Vázquez-González, M., Liao, W.-C., Cazelles, R., Wang, S., Yu, X., Gutkin, V., Willner, I., 2017. ACS Nano 11, 3247–3253.
Wang, S., Cazelles, R., Liao, W.-C., Vázquez-González, M., Zoabi, A., Abu-Reziq, R., Willner, I., 2017. Nano Lett. 17, 2043–2048.
Wang, Z.W., Zhang, J., Guo, Y., Wu, X.Y., Yang, W.J., Xu, L.J., Chen, J.H., Fu, F.F., 2013. Biosens. Bioelectron. 45, 108–113.
Watanabe, R., Matsushima, R., Harada, T., Oikawa, H., Murata, M., Suzuki, T., 2013. Food Addit. Contam.: Part A 30, 1351–1357.
Wei, H., Wang, E., 2008. Anal. Chem. 80, 2250–2254.
Wharton, R.E., Feyereisen, M.C., Gonzalez, A.L., Abbott, N.L., Hamelin, E.I., Johnson, R.C., 2017. Toxicon 133, 110e115.
Wiese, M., D'Agostino, P.M., Mihali, T.K., Moffitt, M.C., Neilan, B.A., 2010. Mar. Drugs 8, 2185–2211.
Yakes, B.J., Prezioso, S., Haughey, S.A., Campbell, K., El-liott, C.T., DeGrasse, S.L., 2011. Sens. Actuators B: Chem. 156, 805–811.
Zhang, J., Wu, X.Y., Yang, W.J., Chen, J.H., Fu, F.F., 2013. Chem. Commun. 49, 996–999.
Zhuo, L.-Y., Yin, Y.-C., Fu, W.-S., Qiu, B., Lin, Z.-Y., Yang, Y.-Q., Zheng, L.-M., Li, J.-R., Chen, G.-N., 2013. Food Chem. 137, 115–121.